Leadership in Sustainable Infrastructure

Leadership en Infrastructures Durables

Vancouver, Canada

May 31 – June 3, 2017/ *Mai 31 – Juin 3, 2017*

FATIGUE - LIFE PREDICTION OF SHEAR STUD USING FINITE ELEMENT ANALYSIS

Mia, Md M.[1] and Bhowmick, Anjan[2,3]
[1] Concordia University, Canada
[2] Concordia University, Canada
[3] anjan.bhowmick@concordia.ca

Abstract: Steel-concrete composite beams are widely used in bridges. The longitudinal shear forces developed at the interface between concrete deck and steel girder is transferred mostly by shear studs. Among different types of shear studs, headed shear stud is most commonly used in practice. In bridges, these shear studs are subjected to rapidly fluctuating stresses which may result in fatigue failure during the lifetime of the structure. Thus, the fatigue resistance of shear studs in composite beams is significant for the safe of whole structure and needs to be well investigated. The aim of this paper is to investigate the fatigue behavior of headed shear studs. A detailed nonlinear finite element model (FEM) is developed using commercial software package ABAQUS for predicting fatigue life of shear studs embedded in a solid concrete slab. Both fatigue crack initiation life and crack propagation life are estimated. The developed FE model is validated against test results and an excellent correlation is found. Finally, an extensive parametric study is performed using the validated finite element model to investigate effects of different parameters on fatigue life of headed shear stud.

1. INTRODUCTION

To join concrete deck and steel superstructure, providing a mechanism for shear transfer across steel-concrete interface, it is advantageous to use shear connectors. Various types of shear connectors such as headed stud shear connectors, channel connectors, block with hoops connectors, post-installed shear connectors, T connectors, perfobond rib connectors, T-perfobond connectors, crestbond connectors have been proposed since 1940's. Among different types of shear connectors, headed shear stud connectors are most common and widely used in steel-concrete composite bridges. The common advantage of this type of shear stud connector is that welding is very fast and it anchors well in concrete (Xie et. al. 2011). Shear studs are often subjected to repeated loadings and these repeated loads can initiate micro-cracks in stud materials which may propagate with the continued application of cyclic stress. This process is known as fatigue. Fatigue failure can be dangerous since it occurs suddenly without significant prior deformations. One of the major drawbacks of headed shear stud connectors is that they are very sensitive to fatigue and thus, care must be taken if used in fatigue prone sites. Fatigue problem of shear studs has been paid a great attention in recent years. The fatigue resistance of headed shear stud is best determined through testing which is very expensive and time-consuming. It is often impractical, or sometimes impossible, to test full-size structural components. As a result, analytical prediction models are often required as an alternative means. In this paper, a three-dimensional FE model has been developed using ABAQUS for predicting fatigue life of shear stud. Both crack initiation life and crack propagation life have been estimated using the developed FE model and an extensive parametric study is conducted to shed more light on fatigue behavior of headed shear studs embedded in steel-concrete composite bridges. Although, the focus of this paper is to study the fatigue failure of shear stud component, concrete damage plasticity is defined in the developed FE model to find out the effects of concrete strength on fatigue life of shear stud.

2. LITERATURE REVIEW

2.1 Previous Works

The fatigue formula of American Association of State Highway and Transportation Officials (AASHTO LRFD) and Canadian Highway Bridge Design Code (CHBDC) are based on single sided push-out test results on 19 mm studs performed by Slutter and Fisher (1966) at Leigh University, Pennsylvania. They tested 26 samples containing 19 mm studs under constant amplitude stress cycles ranging from 55 MPa to 138 MPa and it was reported that fatigue life is a function of stress range and the peak load in fatigue design is insignificant. The effect of minimum stress was found to be significant only in case of stress reversals. Hirokazu et al. (1990) proposed an equation for fatigue life of shear studs from 45 fatigue test data. In their proposed equation, in addition to shear stress amplitude, geometrical dimensions of studs and concrete compressive strength were also related to the fatigue life of shear studs. Lee et al. (2005) studied the fatigue property of large diameter shear studs subjected to low cycle fatigue load and concluded that the fatigue life of larger shear studs is lower than the provisions of European code (EC 4). Mundie (2011) performed twelve push-out tests to evaluate AASHTO LRFD fatigue strength equation**.** It was reported that AASHTO LRFD fatigue strength equation significantly underestimates the fatigue life of shear studs. To study the fatigue behavior of shear stud near the constant amplitude fatigue limit (CAFL), Ovuoba and Prinz (2016) conducted tests on six composite push-out specimens and an underestimation by AASHTO LRFD was reported.

2.2 Fatigue Design Specifications

AASHTO LRFD uses the following Equation 1 to relate stress range and fatigue life which is based on the research work of Slutter and Fisher (1966), as mentioned earlier.

[1] $\Delta\tau = 303 - 37.6\,\log\mathrm{N}$

where N is the number of cycles to failure and $\Delta\tau$ is the stress range in MPa. It is important to note here that AASHTO LRFD uses log-linear curve for fatigue life prediction. CSA S6-14 has made modification to the fatigue requirement of shear stud, based on the work of Zhang (2007), to be consistent with that of other fatigue details (C10.17.2.7 of CSA S6-14). In the work of Zhang (2007), a regression analysis was carried out on a large collection of push-out test data carried by previous researchers and log-log relationship is found to approximate closely if fatigue detail category D is considered. It is important to note that the endurance limit does not change for this fatigue detail category. According to CSA S6-14, the fatigue life can be calculated by Equation 2.

[2] $\mathrm{N} = \frac{\gamma}{(\Delta\tau)^{\mathrm{m}}}$

where N is the number of cycles, γ is the fatigue life constant, m is the slope of the design curve (as given 3) and $\Delta\tau$ is the stress range. Eurocode-4 specifies the following Equation 3 for fatigue strength of an automatically welded headed stud:

[3] $(\Delta\tau_{\mathrm{R}})^{\mathrm{m}}\mathrm{N}_{\mathrm{R}} = (\Delta\tau_{\mathrm{c}})^{\mathrm{m}}\mathrm{N}_{\mathrm{c}}$

where N_{R} is the number of stress-range cycles, $\Delta\tau_{\mathrm{R}}$ is the stress range, $\Delta\tau_{\mathrm{c}}$ is the reference value at 2 million cycles with $\Delta\tau_{\mathrm{c}}$ equal to 95 MPa, m is the slope of the fatigue strength curve and usually taken as 8.

2.3 Fatigue Life Prediction Techniques

There are two basic approaches that are used to calculate total number of cycles a component can sustain before failure: use of $\Delta\sigma$ – N curves and fracture mechanics approach. In this paper, fracture mechanics approach is used to predict total fatigue life. Fracture mechanics is a part of engineering discipline which deals with the crack growth and there are three stages of crack growth. These are crack initiation stage, stable crack propagation stage and unstable crack propagation stage. The total fatigue life is the sum of crack initiation and crack propagation life. Crack initiation life is calculated using empirical correlation approach and stable crack propagation life is calculated using linear elastic fracture mechanics (LEFM) approach. In the empirical correlation approach, different empirical damage parameters, D, are used to correlate with the N, total number of cycles before failure and it is divided into three categories: a) Stress-based method, b) Strain-based method, c) Energy-based method. The strain-based method is widely used for calculating fatigue crack initiation life and it is used in this study. The following Equation 4 proposed by Smith et al. (1970) is used to calculate crack initiation life,

[4] $$\frac{\Delta\varepsilon}{2} = \frac{(\sigma'_f)^2}{\sigma_{max}E}(N_{init})^{2b} + \frac{\sigma'_f\,\varepsilon'_f}{\sigma_{max}}(N_{init})^{b+c}$$

where $\frac{\Delta\varepsilon}{2}$ is the strain range, σ_{max} is the maximum local stress accounting for plasticity, E is the modulus of elasticity, σ'_f is fatigue strength coefficient, ε'_f is fatigue ductility coefficient, b and c are fatigue strength exponent and fatigue ductility exponent respectively and N_{init} is the crack initiation life. Once the crack is initiated, it starts to propagate with the subsequent load cycles. In this stage, crack front grows more and more until failure occurs. According to Paris (1963), the logarithm of crack growth rate, da/dN is proportional to logarithm of stress intensity factor range, ΔK and can be expressed as Equation 5.

[5] $$da/dN = C\,(\Delta K)^m$$

where C and m are material constants. It has been observed that crack does not propagate if stress intensity is less than a certain value known as threshold stress intensity factor range, ΔK_{th}**.** Equation 6 is used in this paper to estimate crack propagation life,

[6] $$N_{prop} = \int_{a_o}^{a_f}\frac{da}{C\,(\Delta K^{\,m} - \Delta K_{th}{}^{m})}$$

where a_o and a_f are the initial and final crack sizes respectively. As per guidelines of ASTM standard E647 (ASTM 2000)**,** ΔK can be taken as $\Delta K = K_{max}$ if only tension portion of stress cycles are considered.

3. FINITE ELEMENT MODELING

3.1 Model Geometry

To develop a three-dimensional FE model for the prediction of fatigue life, the push-out specimen of Lee et al. (2005) has been used and the essential components of push-out specimen, such as concrete slab, steel beam, shear stud and rebar are modeled with the help of general purpose finite element software ABAQUS. The thickness of steel beam and concrete slab are 14 mm and 200 mm respectively. Due to the symmetry of push-out specimen, a quarter of the whole model marked in Figure 1(a) has been used.

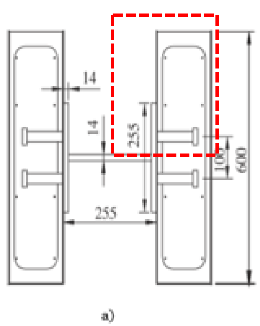

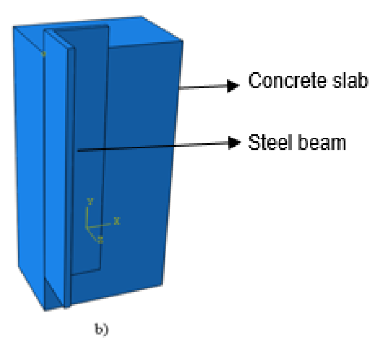

Figure 1: Push-out Specimen; a) Geometry of Model, b) Quarter of Whole Model

The headed shear stud in the push-out specimen is of 25 mm diameter. The overall height of stud is 155 mm and stud head dia and head height are 38 and 11 mm respectively. Welding of the shear stud is modeled with weld having weld collar height of 7 mm and weld base diameter of 31 mm. Figure 2 shows the shear stud used for the development of FE model.

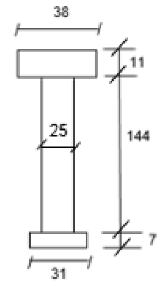

Figure 2: Dimensions of Shear Stud used in FE Analysis

3.2 Contact and Interaction

In order to simulate proper test condition, it is very important to use proper constraint between different parts of the push-out specimen in FE analysis. The nodes of the concrete slab and steel beam around the studs are constrained to the surfaces of shear studs by using tie constraint. In Abaqus, it is necessary to define master and slave surfaces. Shear studs have been selected as master surface and concrete slab as slave. Surface-to-surface discretization method has been used to get more accurate results in the time of defining tie constraint between the pair of surfaces. Figure 3 shows the surfaces used for tie constraint definition,

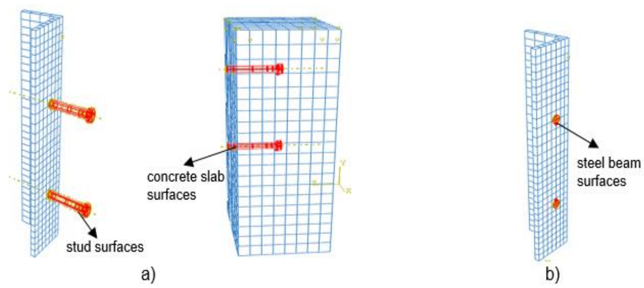

Figure 3: Constraints used in FE analysis; (a) surfaces in tie constraint between concrete slab-stud, (b) surfaces in tie constraint between steel beam and shear stud

A frictionless interaction with penalty contact and hard formulation is used to represent proper test condition in the definition of steel beam-concrete slab interaction. For applying load, load control procedure is followed. To do so, MPC constraint has been used between load surfaces (top surface of steel beam) and a reference point. The MPC constraint used to ensure uniform distribution of load is shown in Figure 4.

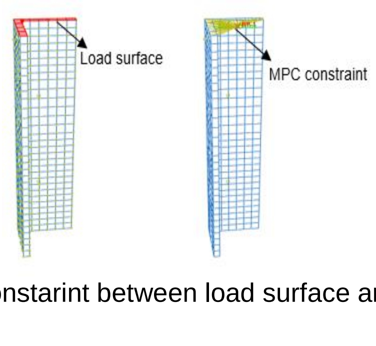

Figure 4: MPC constarint between load surface and reference point

3.3 Boundary Condition

The X-axis symmetric boundary condition (BC) is applied to surface 1 and all the nodes lying in surface-1 are restricted from moving in X-direction and rotation about Y and Z axis are restrained as shown in

Figure 5. The Z-axis symmetric BC is applied to the middle of the steel beam web so that all the nodes of steel beam web are restrained in Z-direction and rotation about X and Y axis are also restrained. All translational and rotational movements are restrained at the bottom surface of concrete slab.

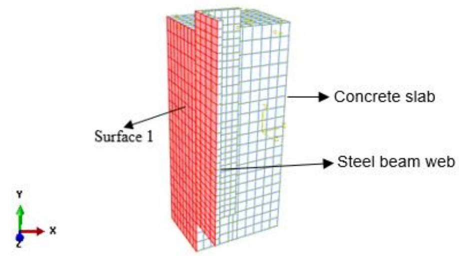

Figure 5: Boundary Condition for FE model

3.4 FE Mesh

To obtain accurate results from finite element analysis, three-dimesional solid elements (hexahedrals) are used to model the push-out components provided they are not distorted. Solid elements can be used for both linear and complex non-linear simulations involving contact, plasticity and large deformations (Karlsson and Sonrensen 2006d). For concrete slab, steel beam and headed shear studs, three-dimensional eight-node element (C3D8R) was selected and T3D2 truss element with linear approximation of displacement was used for rebars. T3D2 element has two nodes and three translational degrees of freedom.

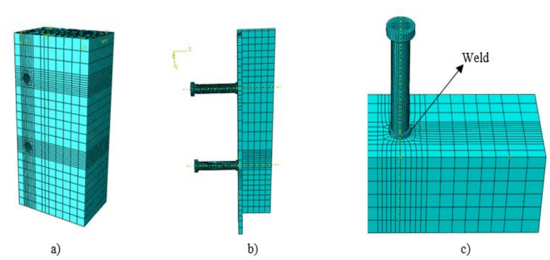

Figure 6: Mesh of the Model; a) Concrete Slab, b) Steel Beam with Stud, c) Shear Stud with Weld

3.5 Material Properties

The yield and ultimate strength of headed shear stud were 353 MPa and 426 MPa respectively as was used in test of Lee et al.(2005). The nonlinear plastic behavior of shear stud is introduced in FE model using a multi-linear isotropic hardening model and Ramberg-Osgood parameters, K' and n' as shown in Equation 7. The value of K' and n' has been collected from the structural engineering report of Josi and Grondin (2010).

[7] $\varepsilon = \frac{\sigma}{E} + \left(\frac{\sigma}{k'}\right)^{n'}$

where K' and n' are 727 MPa and 0.15 respectively. For both structural and reinforcement steel, bi-linear stress-strain relationships have been assumed representing a simple elastic-plastic model. Poisson’s ratio was taken as 0.3 for structural and reinforcement steel material. The yield strength of reinforcement steel and structural steel was 400 and 320 MPa respectively. In this paper, the uniaxial stress-strain curve of concrete presented by Nguyen and Kim (2009) has been used with slight modifications. There are three parts in this stress-strain curve. In the first part, stress increases linearly up to 0.4 f'c, where $f'c$ is the 28-days concrete cylindical compressive strength. The second part of the curve is an ascending part up to $0.9f'c$. The peak stress is used as $0.9f'c$ as suggested in CSA A23.3-14. The strain $\varepsilon 1$ related to $0.9f'c$ has been taken as 0.0022 and Poisson’s ratio is taken as 0.2 for concrete. The third part of the curve is a descending part up to r f'c where the value of r is the reduction factor and the value of r is taken from the study of Ellobody et al. (2006) and the ultimate strain of concrete is used as 0.0035 as suggested by CSA A23.3-14. For concrete in tension, the tensile stress is assumed to increase linearly till crack and then tensile stress decreases linearly to zero. The strain at zero tensile stress is taken as 0.005 as used by Nguyen and Kim (2009).

4. FATIGUE LIFE PREDICTION PROCEDURE

4.1 Crack Initiation Life

Lee et al. (2005) tested 12 specimens for fatigue life investigation on three different diameters: 25, 27 and 30 mm. In this paper, four specimens of 25 mm diameter have been investigated and an approach for fatigue life prediction of shear stud using push-out specimen has been proposed. Table 1 shows the maximum and minimum loads and stress ranges used in FE analysis.

Table 1: Load and Stress Ranges for 25 mm Shear Stud

Specimen	Concrete Strength (MPa)	Maximum Load (kN)	Minimum Load (kN)	Stress range (MPa)
FT25A2	30	73.6	0	150
FT25A3	30	83.4	0	170
FT25B1	40	63.8	0	130
FT25B2	40	73.6	0	150

ABAQUS dynamic explicit formulation is adopted for the analysis in this study. ABAQUS explicit formulation is popularly used for problems of impact, progressive damage and failure of material (Nguyen and Kim 2009). It has been applied in many problems such as crack and failure of concrete material (William et al. 2005). Dynamic explicit is a time control method since the global mass and stiffness matrices need not be formed and inverted resulting relatively inexpensive increment compared to implicit analysis. It is important to note here that crack is not explicitely modeled in the FE model. Rather, it is assumed that crack will generate in highly stressed area. The location of highly stressed area can be identified from FE analysis. In the first time step, the model is fully loaded to maximum load. The load is then reduced to minimum load in the second time step, and finally it is reloaded to maximum load again in time step 3. After time step 2 and 3, the nominal strains in the X direction are recorded from the output file and the maximum nominal stress in X direction in time step 3 is also recorded. The critical location of push-out specimen was reported at the base of the weld collar (Lee et al. 2005) which can also be seen from Figure 7. Once strain and maximum stress at critical location are obtained, crack initiation life is calculated using Equation 4. The crack initiation properties are collected from the report of Wang (2010).

4.2 Crack Propagation Life

As mentioned earlier, Equation 6 is used to predict crack propagation life and the values of ΔK_{th}, C and m are collected from the report of Wang (2010) which are 100 MPa√mm, 2.71x10^{-13} and 3 respectively. For crack propaagtion life, it is very important to identify the fatigue failure modes.

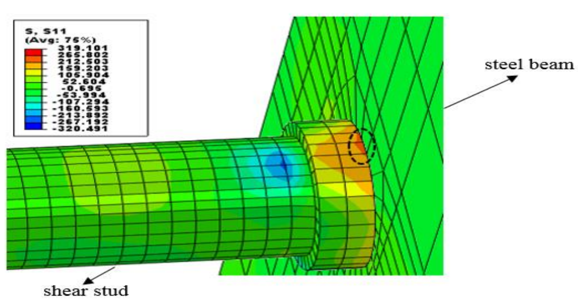

Figure 7: Critical Location of Shear Stud at the Base of Weld Collar

Figure 8 shows the two common fatigue failure modes, Mode A, in which crack initiates at the top of the weld collar and then propagates along the stud-weld interface; in Mode B, the crack initiates at the base of the weld collar and propagtes untill it reaches to the base of the weld collar again through the joist material. In the test of Lee et al. (2005), Mode B was reported which has been used in this paper.

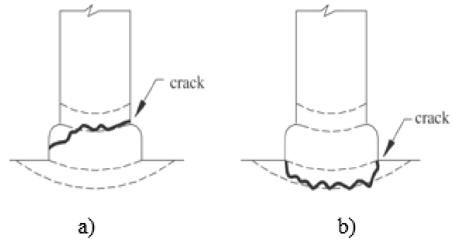

Figure 8: Fatigue Failure Mode; a) Mode A, b) Mode B

For prediction of crack propagation life, it is needed to use initial and final crack size. The approximate initial crack size is normally taken as engineering crack size which is visible to naked eye and normally 1 to 5 mm (Chen et al. 2005). If the crack size is too small, then small crack effects may need to be considered and linear elastic fracture mechanics (LEFM) method may not apply (Ellyin 1997). In this paper, intitial crack size 1 mm gives a good correlation with the test value. For final crack size, the weld base diameter of 31 mm has been taken considering failure mode B shown in Figure 8. The stress intensity factor, k used in Equation 6 is determnined by the following Equation 8 (Dowling 2007).

[8] $K = 1.12\, S \sqrt{(\pi a)}$

where, S is the nominal stress and a is the crack size.

5. RESULTS

5.1 Comparison of FE Analysis Results

The fatigue life of the four specimens obtained from FE analysis using the above-mentioned procedure are given below in Table 2. An excellent correlation with test results of Lee et al (2005) is observed.

Table 2: Comparison of Fatigue Life

Specimen	Fatigue life, Test	Fatigue Life, FEA
FT25A2	44827	50586
FT25A3	60000	38646
FT25B1	387209	355439
FT25B2	61063	61351

A comparison between FEA results and design values according to CSA S6-14, EC 4 and AASHTO LRFD are summarized in table 3 and Figure 9.

Table 3: Comparison of Fatigue Life with Design Standards

Specimen	Fatigue Life, FEA	Fatigue Life, EC4	Fatigue life, CSA S6-14	Fatigue Life, AASHTO LRFD
FT25A2	50586	51772	213630	11726
FT25A3	38646	19021	146754	3460
FT25B1	355439	162657	328175	40086
FT25B2	61351	51772	213630	11726

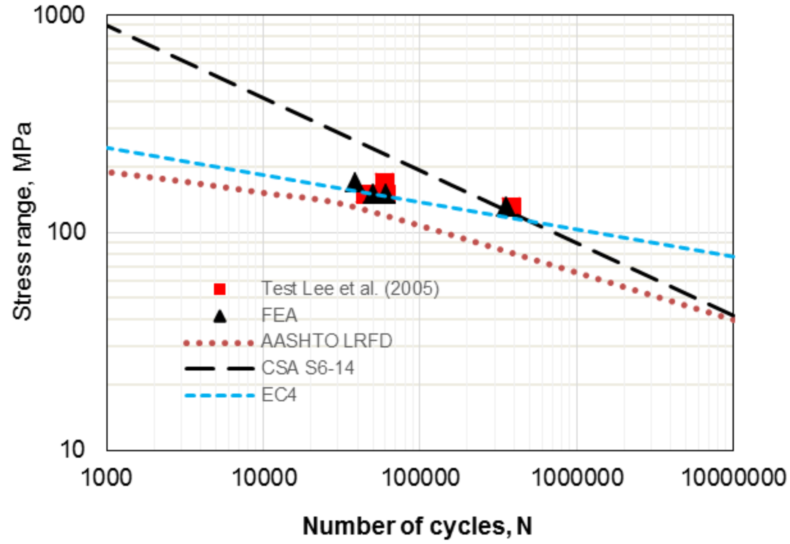

Figure 9: S-N curves

5.2 Parametric Study

In order to understand the influence of several parameters such as stud spacing, concrete slab thickness, concrete strength on fatigue life of shear stud, a parametric study is performed.

5.2.1 Stud Spacing

To investigate the effects of stud spacings on fatigue life, three different shear stud spacings (200, 250 and 300 mm) are considered. Figure 10 shows the variation of fatigue life with the change of stud spacing for specimen FT25A2. As can be seen from Table 4, a decrease in the fatigue life is observed with the increase of stud spacing for all fatigue specimen.

Table 4: Fatigue Life Variation with Stud Spacing

Stud Spacing	Fatigue Life		
mm	FT25A2	FT25A3	FT25B1
200	134360	89275	376015
250	50586	38646	355439
300	22545	17143	231393

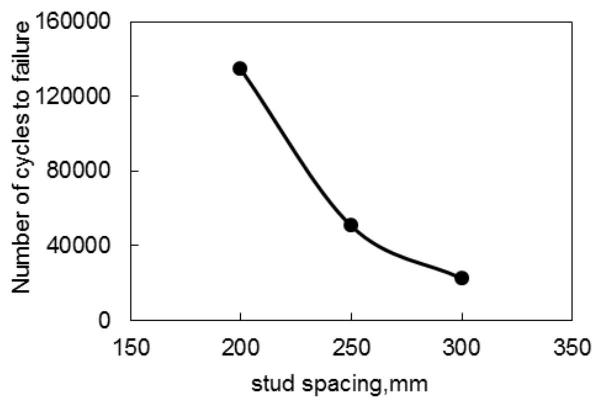

Figure 10: Stud Spacing Effects on Fatigue Life (FT25A2)

5.2.2 Slab Thickness

To investigate the slab thickness effects on fatigue life, parametrc study is conducted with three different slab thicknesses (200, 250 and 300 mm). The results are shown in Table 5. It is observed that fatigue life decreases with the increase of slab thickness. This is due to the increase of shear forces which leads to the reduction of fatigue life.

Table 5: Fatigue Life Variation with Slab Thickness

Stud Spacing mm	Fatigue Life FT25A2	FT25A3	FT25B1
200	50586	38646	355439
250	44593	21550	198937
300	32434	18214	101339

5.2.3 Concrete Strength

From the tests, the strength of concrete was found to have minor effects on fatigue life of shear stud (Slutter el al. 1966). The mean compressive strength of all cylinders was around 30 MPa in their test. Now-a-days, higher concrete strenth is used in steel-concrete composite bridges. Thus, another parameter, concrete strength is taken to investigate it's effects on fatigue life. Five different concrete cylindrical compressive strengths (25, 30, 35, 40 and 45 MPa) are chosen. To account the effects of concrete strength, concrete damage plasticity is defined in the developed FE model. Results from analysis are shown in Table 6 and Figure 11. It can be observed that an increase in concrete strength leads to an increase in fatigue life but the increase is not significant.

Table 6: Fatigue Life Variation with concrete strength

Concrete Strength MPa	Fatigue Life FT25A2	FT25A3	FT25B1
25	41478	32919	296636
30	50586	38646	309500
35	55608	47197	318768
40	61351	66031	355439
45	62184	69791	450018

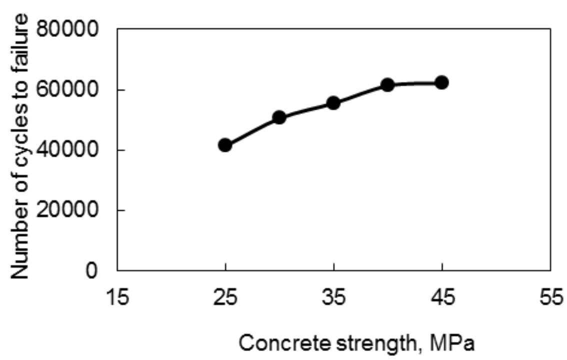

Figure 11: Concrete Strength Effects on Fatigue Life (FT25A2)

6. CONCLUSION

A finite element based approach using the push-out test is proposed for fatigue life estimation of shear studs. Both crack initiation life and crack propagation life are estimated and a good correlation is found with test results. When FE analysis results are compared with design code of practises, such as EC 4, CSA S6-14 and AASHTO LRFD, a significant underestimation is found in case of AASHTO LRFD, while notable amount of overestimation is seen in case of CSA S6-14 demanding more study in this area. Finally, the parametric study reveals that the effect of concrete strength on fatigue life is insignificant.

Acknowledgements

Funding for this research project is provided by the Faculty of Engineering and Computer Science, Concordia University, Montreal, Canada and the Natural Sciences and Engineering Research Council of Canada.

7. REFERENCES

AASHTO (American Association of State Highway and Transportation Officials) 2012. *AASHTO LRFD Bridge Design Specifications.*

ASTM Designation E 647-00: *Standard Test Method for Measurement of Fatigue Crack Growth Rates.* American Society for Testing and Materials, Philadelphia, USA.

Chen, H., Grondin, G.Y. and Driver, R.G. 2005. *Fatigue Resistance of High Performance Steel*. University of Alberta, Edmonton, Alberta, Canada.

CSA (Canadian Standards Association) 2014. *CAN/CSA-S6-14, Canadian Highway Bridge Design Code.*

Dowling, N.E. 2007. *Mechanical Behavior of Materials: Engineering Methods for Deformation, Fracture, and Fatigue*. 3rd ed., Pearson Prentice Hall, Upper Saddle River, USA.

Ellobody, E., Young, B. and Lam, D. 2006. Behaviour of normal and high strength concrete-filled compact steel tube circular stub columns. *Journal of Constructional Steel Research*, **62**(7): 706-715.

Eurocode 4. (1997). *ENV 1994-2 Eurocode-4: "Design of composite steel and concrete structures, Part 2: Composite bridges*." European Committee for Standardization (CEN), Brussels, Belgium.

Ellyin, F. 1997. *Fatigue Damage, Crack Growth and Life Prediction*. Chapman & Hall, London, UK.

Hirokazu, H., Shigeyuki, M. and Fukumoto, Y. (1990). Static and fatigue strength of studs. *Labse Symposium*, Brussels, **60**:197-202.

Josi, G. and Grondin, G.Y. 2010. *Reliability-Based Management of Fatigue Failures*. University of Alberta, Edmonton, Alberta, Canada.

Karlsson and Sonrensen. 2006d. *ABAQUS user's manual volume IV: Element,* Pawtucket, Rhode Island, Hibbit Publication.

Lee, P.G., Shim, C.S. and Chang, S.P. 2005. Static and fatigue behavior of large stud shear connectors for steel-concrete composite bridges. *Journal of Constructional Steel Research*, **61**(9): 1270-1285.

Mundie, D.L. 2011. *Fatigue Testing and Design of Large Diameter Shear Studs Used in Highway Bridges.* Auburn University, Auburn, Alabama, USA.

Nguyen, H.T. and Kim, S.E. 2009. Finite element modeling of push-out tests for large stud shear connectors. *Journal of Constructional Steel Research,* **65**(10-11): 1909-1920.

Ovuoba, B. and Prinz, G.S. 2016. Fatigue Capacity of Headed Shear Studs in Composite Bridge Girders. *Journal of Bridge Engineering*, **21**(12): 01-09.

Paris, P. and Erdogan, F. 1963. A Critical Analysis of Crack Propagation Laws. *Transactions of the ASME*, **85**(4): 528-534.

Slutter, R. G. and Fisher, J.W. 1966. *Fatigue Strength of Shear Connectors*. Lehigh University Institute of Research, Bethlehem, PA, USA.

Smith, K.N., Watson, P. and Topper, T.H. 1970. A Stress-Strain Function for the Fatigue of Materials. *Journal of Materials*, **5**(4): 767-778.

Wang, Y. 2010. *Fatigue Repair Technique Investigation - Hole Drilling and Expansion Method.* PhD Thesis, Department of Civil Engineering, University of Alberta, Edmonton, Canada.

William, A., John, L. and Conrad, I. 2005. Perforation of composite floor. *5th European LS-DYNA users conference*, Birmingham:3c-56.

Xie, E. and Valente, M.I.B. 2011. *Fatigue Strength of Shear Connectors*. University of Minho, Guimaraes, Portugal.